Effects of the Molecular Structure of Malodor Substances and Their Masking on 1,2-Dioleoyl-*sn*-glycero-3-phosphocholine Molecular Layers

Mai Yotsumoto[1], *Risa Fujita*[1], *Muneyuki Matsuo*[1,2], *Shinobu Nakanishi*[3], *Mitsuhiro Denda*[4], *Satoshi Nakata*[1,*]

1. Graduate School of Integrated Sciences of Life, Hiroshima University, Kagamiyama 1-3-1, Higashi-Hiroshima, Hiroshima 739-8526, Japan
2. Graduate School of Arts and Sciences, The University of Tokyo, 3-8-1 Komaba, Meguro-ku, Tokyo, 153-8902, Japan
3. Shiseido Global Innovation Center, 1-2-11, Takashima-cho, Nishi-ku, Yokohama, Kanagawa 220-0011, Japan
4. Meiji University, Institute for Advanced Study of Mathematical Sciences, 8F High-Rise Wing, Nakano Campus, Meiji University, 4-21-1 Nakano, Nakano-ku, Tokyo, 164-8525, Japan

Received date:

*To whom correspondence should be addressed.

E-mail: nakatas@hiroshima-u.ac.jp, Tel/fax number: +81-82-424-7409

Keywords: monolayer, phospholipid, malodor substances, masking

Abstract

Certain odors have not only been shown to cause health problems and stress but also to affect the skin barrier function. Therefore, it is important to understand olfactory masking in order to develop effective fragrances to mask bad odors. However, olfaction and olfactory masking mechanisms are not yet fully understood. To understand the mechanism of the masking effect that has been studied, the responses of several target substances (TS)-1,2-dioleoyl-*sn*-glycero-3-phosphocholine (DOPC) mixed molecular layers to odorants (OD) were examined as a simple experimental model of epithelial-cellular membranes injured by TS molecules. Here, we examined *trans*-2-nonenal, 1-nonanal, *trans*-2-decenal, and 1-decanal as TS molecules to clarify the effects of double bonds and hydrocarbon chain length on the phospholipid molecular layer. In addition, benzaldehyde and cyclohexanecarboxaldehyde were utilized as OD to clarify the masking effect of the aromatic ring. Surface pressure (Π) - area (A) isotherms were measured to clarify the adsorption or desorption of TS and OD molecules on the DOPC molecular layer. In addition, Fourier-transform infrared spectroscopy was performed to clarify the interactions between DOPC, TS, and OD molecules. We found that TS molecules with and without double bonds had different effects on the DOPC molecular layer and that molecules with shorter chain lengths had greater effects on the DOPC molecular layer. Furthermore, OD with aromatic rings counteracted the effects of TS molecules. Based on this research, not only a detailed mechanism by which odor molecules affect lipid membranes without mediating olfactory receptors is elucidated but also more effective OD molecules with masking effects are proposed.

INTRODUCTION

Daily odors in living spaces can cause health hazards and increase stress.[1–6] *Trans*-2-nonenal (NE), generated by the oxidative degradation of ω seven unsaturated fatty acids at the surface of the skin in an aging-related manner,[7] has an unpleasant greasy odor.[8] A previous report demonstrated that, among body odor components, only NE in skin surface stratum corneum obviously increases with aging[7], and another report indicated that the recovery of the stratum corneum after its disruption is delayed with aging.[9] Nakanishi *et al.* reported that NE is cytotoxic to human keratinocytes and induces abnormal cornification.[10]

Masking of odors plays an important role in preventing the various harms caused by odors.[11–14] Odorant masking is a phenomenon in which a malodor is no longer perceived when smelled with specific odorants. One of the masking mechanisms is olfactory receptor antagonism. However, chemotransduction-independent suppression of voltage-gated currents by odorants has been observed in olfactory neurons.[15] Nakanishi *et al*. also reported that the induction of apoptosis and reduction of viability of human keratinocytes by NE is blocked by specific masking odors, even though keratinocytes are not olfactory cells.[10]

Phospholipid artificial membrane is used as model cell membrane to investigate

the mechanism of cell response since it is difficult to factor out intrinsic elements and their nature on the mechanism of chemical sensation in living organisms due to their complexity.[16-20] Indeed, interactions between chemical species and functional groups in phospholipid artificial membranes have been reported to be associated with barrier homeostasis of cellular membranes in skin.[21] It has also been reported that membrane fluidity of liposomes is affected by odorants.[22-25] We recently evaluated the interaction between odorant (OD) molecules and phospholipid molecular layers based on the spectroscopies and the surface pressure (Π)-area (A) isotherms.[26] As a result, it was revealed that NE molecules are adsorbed into the 1,2-dioleoyl-*sn*-glycero-3-phosphocholine (DOPC) molecular layer and are desorbed by forming a complex with aromatic OD molecules. In other words, OD molecules with aromatic rings have a masking effect on NE, while OD molecules without aromatic rings have no effect.[26] These studies suggest that NE desorption from membrane is promoted by the interaction between NE and odorants in masking phenomena. However, the relationships between the chemical structures of NE and OD molecules to the response of phospholipid molecules have not yet been clarified.

We investigated the interactions among DOPC as an artificial lipid membrane, target substance (TS), and OD molecules to understand the masking effects. We selected

NE, 1-nonanal (NA), *trans*-2-decenal (DE), and 1-decanal (DA) as TS molecules because these substances are found as unpleasant greasy odors in human sweat.[27] Benzaldehyde (BA), which are selected as candidates for masking odor,[11] and cyclohexanecarboxyaldehyde (CA) as its counterpart substance are abbreviated as OD molecules (Scheme 1). The interactions of DOPC, TS, and OD were characterized by utilizing surface pressure (*Π*)-area (*A*) isotherms and attenuated total reflection Fourier-transform infrared spectrometry (ATR-FT-IR). The interaction among DOPC, TS, and OD verified in this study is consistence with the toxicity and masking effect of keratinocytes for NE and NA. The toxicity and masking effects of other odors, e.g., DE and DA, have not been clarified. This consistency indicates the ability of this systematic model system to predict the cytotoxicity, masking effect, and their mechanisms.

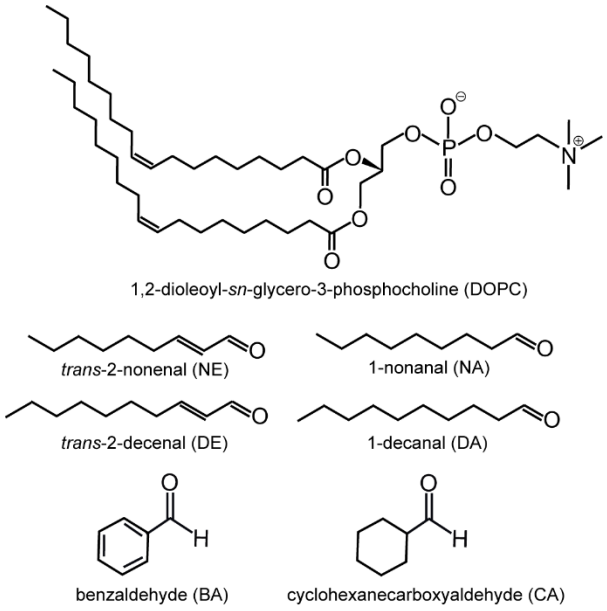

Scheme 1. Chemical structures of compounds utilized in this study.

EXPERIMENTAL

DOPC, NE, NA, DE, DA, BA, and CA were purchased from Sigma-Aldrich (St. Louis, MO, USA). Chloroform was purchased from Nacalai Tesque, Inc. (Kyoto, Japan). The *Π-A* isotherms of DOPC monolayers were obtained utilizing a surface pressure meter (Kyowa Interface Science Co. Ltd., HMB, Saitama, Japan) at 20 ± 1 ℃. 56 μL DOPC chloroform solution (amount of DOPC: 1.62×10^{-8} mol) was gently dropped on water. Water was distilled and purified employing a Millipore Milli-Q filter system (resistance: 18 MΩ cm). The surface area was reduced with a barrier from 210 to 42 cm^2 at a rate of 16.5 cm^2 min^{-1}, that is 17 $Å^2$ $molecule^{-1}$ min^{-1} for the DOPC monolayer. DOPC, TS, and OD molecules were individually dissolved in chloroform to prepare their individual stock solutions. Each chloroform stock solution was developed simultaneously before the compression. The *Π-A* isotherms were independent of injection order of TS and OD. Compression of the monolayer began 5 min after adding the chloroform solution to remove the chloroform from the aqueous surface by evaporation. At least four examinations were performed for each condition to confirm the reproducibility of the *Π-A* isotherm.

ATR-FT-IR spectra were measured employing an FT-IR spectrophotometer (Nicolet Summit FT-IR Spectrometer, Thermo Fisher Scientific Inc. MA) equipped with an attenuated total reflection (ATR) diamond cell (EverestTM Diamond ATR Accessory) at room temperature. For the measurement of the three-component system, 1 μL chloroform solution including DOPC (amount: 1.0×10^{-8} mol), TS molecules (amount: 5.0×10^{-8} mol), and OD molecules (amount: 5.0×10^{-8} mol) was placed on the cell, and the solvent was dried to obtain a laminated film of the mixture. A cover glass (15 × 15 mm) was placed on the laminated film to prevent the volatilization of TS and OD molecules. The spectral resolution and the cumulative number were 1 cm^{-1} and 100, respectively.

RESULTS and DISCUSSION

As for the two-component system, each TS chloroform solution was added to a DOPC monolayer to evaluate the effect of TS molecules on the DOPC monolayer. *Π–A* isotherms of the DOPC monolayer after the addition of TS molecules (NE, NA, DE, and DA) are shown in Figure 1. The compression modulus analysis for Figure 1 is shown in Figure S1. *Π* for the mixture of DOPC-NE molecular layers was higher than that for DOPC alone at $60 < A < 160$ $Å^2$ $molecule^{-1}$ (Figure 1a). NA and DE increased *Π* for the DOPC monolayer at $75 < A < 160$ $Å^2$ $molecule^{-1}$ (Figures 1b and 1c). In contrast, DA did

not change Π for the DOPC molecular layer.

The Π-A isotherms for the three-component systems, that is DOPC-NE-BA, DOPC-NE-CA, DOPC-NA-BA, DOPC-NA-CA, DOPC-DE-BA, DOPC-DE-CA, DOPC-DA-BA, and DOPC-DA-CA, were measured to clarify the characteristic responses of BA and CA to the DOPC-TS molecular layer, as shown in Figure 1. Π for DOPC-NA was increased by adding BA (Figure 1b), but Π for DOPC-NE and DOPC-DE were decreased by the addition of BA (Figures 1a and 1c). In contrast, CA increased slightly Π for DOPC-NE, DOPC-NA, and DOPC-DE (Figures 1a, 1b, and 1c). When CA was added to the DOPC-NA mixed molecular layer, a plateau region in the Π-A isotherm was observed (Figure 1b). Π for DOPC-DA did not change upon adding BA or CA (Figure 1d).

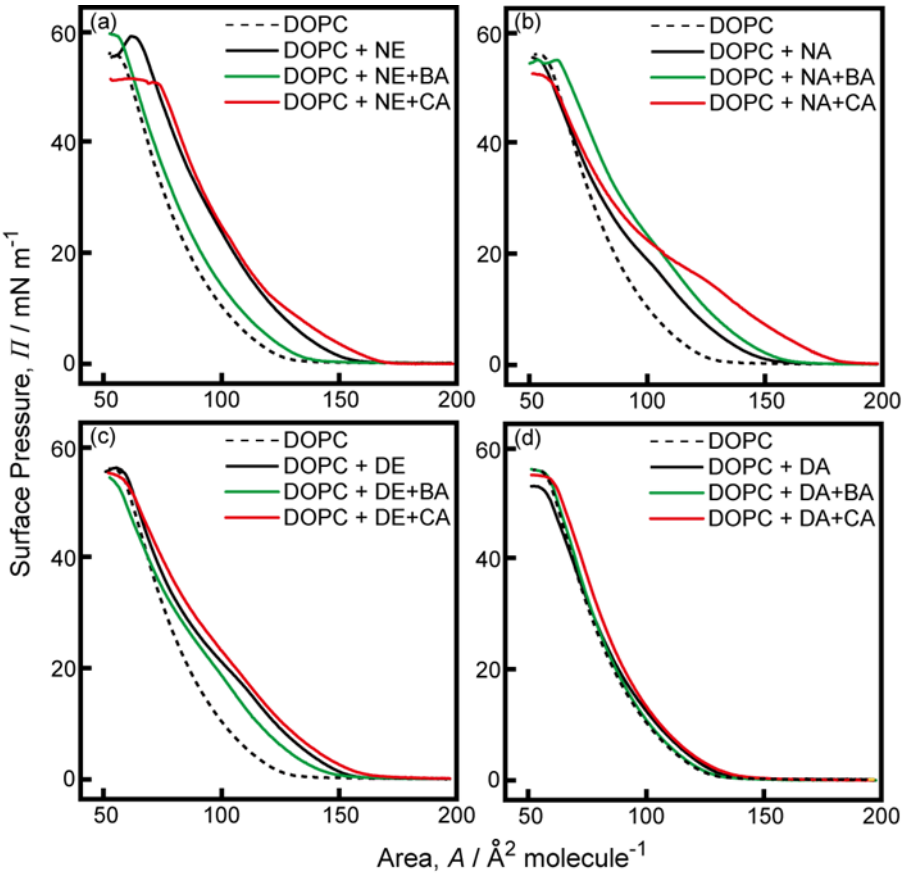

Figure 1. *Π-A* isotherms of DOPC monolayers on water adding TS (black line; (a) NE, (b) NA, (c) DE, (d) DA), and TS plus OD (BA (green line), CA (red line)). Dotted lines denote *Π-A* isotherms of DOPC monolayer without additives. Molar ratios for two- and three-component systems were M_{TS} /M_{DOPC} = 5 and M_{TS} /M_{DOPC} = M_{OD}/M_{DOPC} = 5, respectively, and $M_{DOPC} = 1.62 \times 10^{-8}$ mol, $M_{TS} = M_{OD} = 8.10 \times 10^{-8}$ mol. *A* is the average area per molecule of only DOPC.

Next, we analyzed the *Π-A* isotherms of the DOPC-TS-OD mixtures as a three-component system to evaluate the effects of OD molecules (BA and CA) on the DOPC-TS (NE, NA, DE, and DA) mixed monolayer, as shown in Figure 2. Here, the increase in ΔA (= $A_{DOPC+TS} - A_{DOPC}$ or $A_{DOPC+TS+OD} - A_{DOPC}$) corresponds to the increase in *Π* and was utilized for the reasons (1)–(4). (1) If ΔA for DOPC-TS and DOPC-TS-OD is zero,

TS and OD molecules do not adsorb onto the DOPC molecular layer. (2) If ΔA for DOPC-TS-OD was equal to that of DOPC-TS, the DOPC-TS molecular layer was not sensitive to OD. (3) If ΔA for DOPC-TS-OD was greater than that for DOPC-TS, the OD molecules were adsorbed onto the DOPC-TS mixed molecular layer. (4) If ΔA for DOPC-TS-OD is lower than that for DOPC-TS, adding OD molecules may partially break the DOPC-TS mixed molecular layer. As shown in Figure 2, ΔA for DOPC-NE decreased with the addition of BA (Figure 2a). In contrast, ΔA for DOPC-NA increased with the addition of BA and CA (Figure 2b). The changes in ΔA for DE and DA were smaller than those for NE and NA (Figures 2c and 2d).

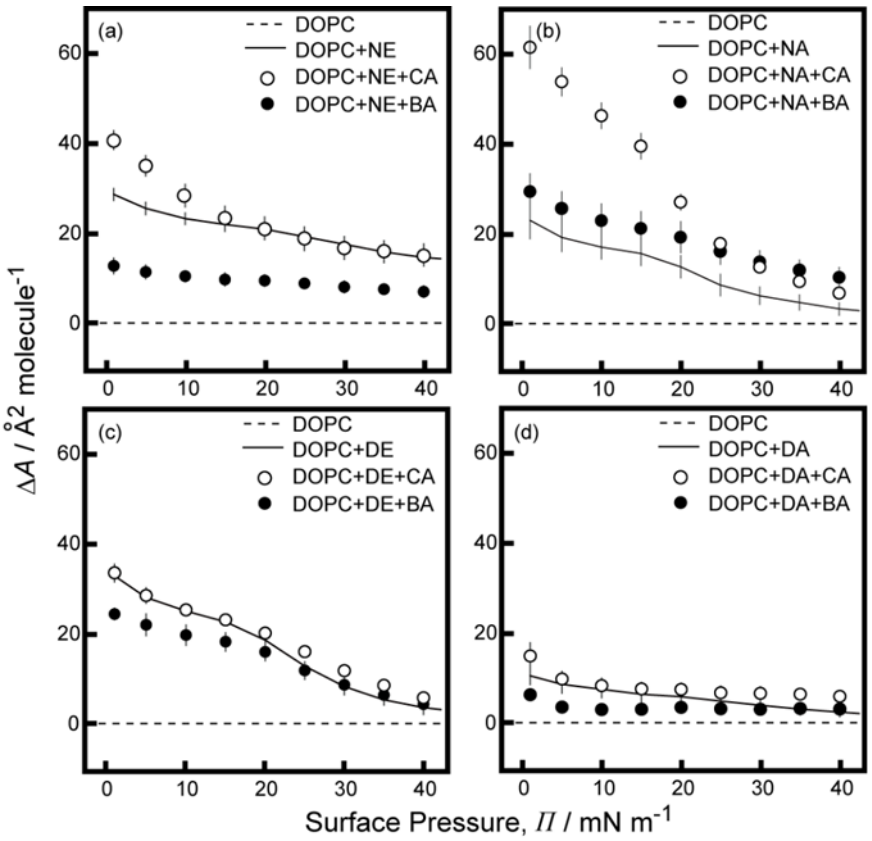

Figure 2. Δ*A* at different values of *Π* for DOPC-TS (solid line) and DOPC-TS-OD (BA (filled circles) and CA (empty circles)) mixtures. These data correspond to those shown in Figure 1. The horizontal dotted line indicates that *A* for the DOPC-TS and DOPC-TS-OD was equal to that for DOPC. Error bars represent the standard deviation from four examinations. These data correspond to those shown in Figure 1.

ATR-FT-IR was utilized to evaluate the intermolecular interactions between DOPC and the additives from the viewpoint of functional groups. Figure 3 presents FT-IR spectra which correspond to PO_2^- antisymmetric stretching vibration mode of DOPC ($\tilde{\nu}$ (PO_2^-)). FT-IR spectra for the DOPC, DOPC-TS, and DOPC-TS-OD mixtures over the wavenumber range of 1000–3500 cm^{-1} are shown in Figure S2. We analyzed the

wavenumber of the peak maxima on $\tilde{\nu}$ (PO_2^-), mixed with additives (DOPC-TS or DOPC-TS-OD) adopting the fitting based on the Gaussian function for several other peaks, i.e., CH_2 wagging and CO-O stretching,[28] as shown in Figure S3. $\tilde{\nu}$ (PO_2^-) (ca. 1240 cm^{-1}) was increased with the addition of NE and DE (Figures 3a1 and 3a3). However, $\tilde{\nu}$ (PO_2^-) did not changed with the addition of NA and DA (Figures 3a2 and 3a4). $\tilde{\nu}$ (PO_2^-) for both the mixtures of DOPC-NE and DOPC-DE were red-shifted by adding BA (Figures 3a1 and 3a3). In contrast, $\tilde{\nu}$ (PO_2^-) for the mixture of DOPC-NE and DOPC-DE slightly blue-shifted and red-shifted with the addition of CA, respectively (Figures 3a1 and 3a3). $\tilde{\nu}$ (PO_2^-) for the mixture of DOPC-NA and DOPC-DA slightly red-shifted with the addition of BA (Figures 3a2). In contrast, $\tilde{\nu}$ (PO_2^-) for the mixture of DOPC-NA and DOPC-DA blue-shifted with the addition of CA (Figures 3a2 and 3a4).

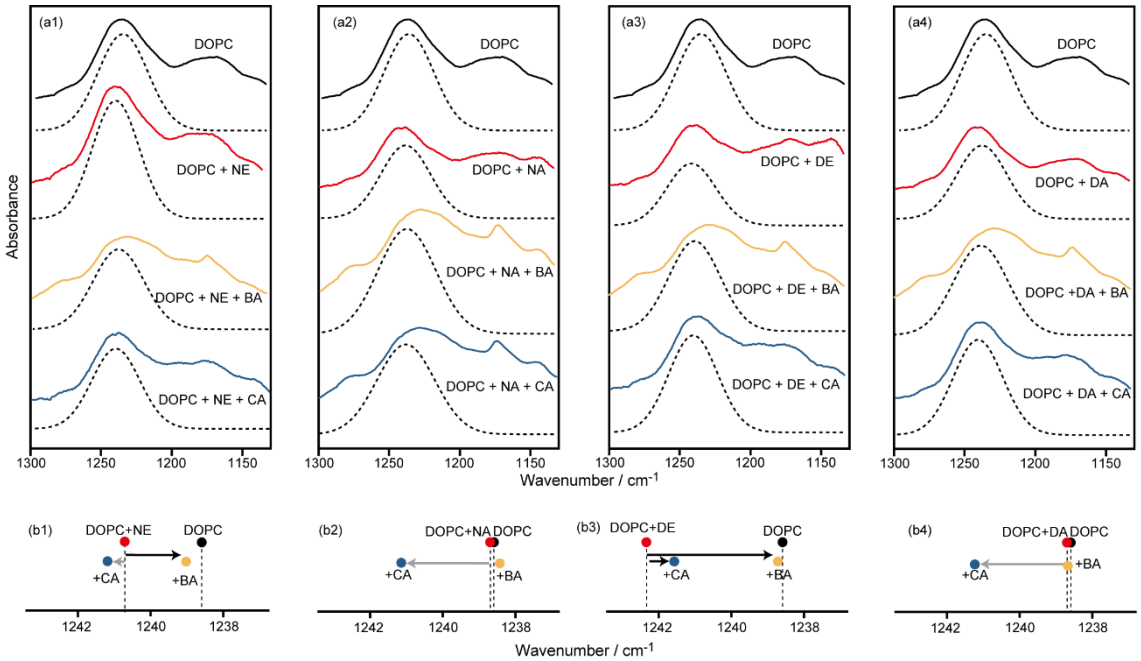

Figure 3. (a) FT-IR spectra presenting the peak region corresponding to PO_2^- antisymmetric stretching region (~1240 cm^{-1}) for DOPC (black line), DOPC-TS (red line), DOPC-TS-BA mixture (yellow line), and DOPC-TS-CA mixture (blue line). Dotted lines were fitting curves corresponding to PO_2^- antisymmetric stretch vibration mode in DOPC. (b) Wavenumbers of IR absorbance peak arising from PO_2^- antisymmetric stretching vibration mode of DOPC for DOPC only, DOPC-TS mixture, and DOPC-TS-OD mixtures (OD: BA and CA, TS: (1) NE, (2) NA, (3) DE, and (4) DA). The black and gray arrows denote red and blue shifts, respectively.

Based on the experimental results mentioned above and related papers,[10, 17–27] we discuss the characteristic responses of TS molecules to the DOPC molecular layer. Π for all the samples utilized, that is, NE, NA, DE, DA, BA, and CA, were maintained at zero for A > 15 $Å^2$ $molecule^{-1}$ (Figure S4). The TS molecules used in this study have a molecular area of ca. 12 $Å^2$ (calculated by Molview). Therefore, the fact that the surface pressure was almost 0 mN m^{-1} at A = 15 $Å^2$ indicates that molecular packing does not

occur neatly and that no monolayer is formed. Regarding the effect of TS molecules on the DOPC molecular layer, the increase in Π for DOPC with the addition of NE, NA, and DE suggests that these molecules are adsorbed onto the DOPC monolayer (Figures 1a, 1b, and 1c). In the case of TS molecules with longer chain lengths, such as DE and DA, the smaller change in Π compared to NE and NA suggests that the DOPC molecular layer is sensitive to the length of the alkyl chain of TS (Figures 1b and 1d). A cell-based study has also reported the importance of an appropriate alkyl chain length for interaction with the lipid membrane.[29] The increase in Π for DOPC with the addition of NE at $60 < A < 160$ Å^2 molecule^{-1} suggests that NE molecules are stably adsorbed on the DOPC molecular layer rather than on NA, i.e., double bonds in the TS molecules are important for adsorption onto the DOPC molecular layer. (Figure 1a). It is consistent with the fact that molecules with double bonds are more likely to adsorb in the phospholipid molecular layer although TS molecules with a double bond have a lower oil-water partition coefficient than those without a double bond. The reason why the plateau characteristic is observed for the Π-A isotherm in the DOPC-NA-CA mixed molecular layer has not been clarified yet.

Next, we focus the ΔA for the Π-A isotherms to evaluate the effects of OD molecules. Larger values of ΔA for DOPC-NE-CA and DOPC-NA-CA than that for

DOPC-NE and DOPC-NA suggest that the CA molecules are additionally adsorbed on the DOPC-NE and DOPC-NA molecular layers (Figures 2a and 2b). We previously reported that for the *Π-A* isotherm of DOPC-OD, *Π* was not changed by the addition of BA but *Π* was increased by the addition of CA.[27] Therefore, CA is easily adsorbed on the DOPC molecular layer. In contrast, the smaller value of ΔA for DOPC-NE-BA and DOPC-DE-BA compared to those for DOPC-NE and DOPC-DE suggest that NE and DE were desorbed from the air–water interface by the addition of BA (Figures 2a and 2c). In addition, because the degree of decrease in ΔA for DOPC-NE is larger than that for DOPC-DE by adding BA, TS molecules with shorter alkyl chain lengths may be easier to desorb into the aqueous phase. ΔA for DOPC-NA-BA is larger than that for DOPC-NA, suggesting additional adsorption of BA molecules on the DOPC-NA mixed molecular layer.

Then, we focus on the peak shift of FT-IR spectra to evaluate the molecular interaction. Blue shifts for $\tilde{\nu}$ (PO_2^-) with the addition of NE and DE (Figures 3a and 3b) suggest that the hydrophilic interaction between DOPC molecules *via* hydrogen bonding of H_2O and PO_2^- group is weakened by the adsorption of either NE or DE onto the DOPC molecular layer. We define $\Delta\ \tilde{\nu}$ (PO_2^-) = $\tilde{\nu}_{\text{DOPC-TS-OD}} - \tilde{\nu}_{\text{DOPC-TS,}}$ to compare between $\tilde{\nu}$ (PO_2^-) of DOPC-TS and DOPC-TS-OD. The negative change of $\Delta\ \tilde{\nu}$ (PO_2^-) for the

DOPC-NE and DOPC-DE mixtures with the addition of BA and the slight changes of Δ $\tilde{\nu}$ (PO_2^-) for DOPC-NE and DOPC-DE mixtures with the addition of CA suggest that the benzene ring of BA is important for the desorption of NE and DE (Figure 3b1 and 3b3). We previously reported that in the FT-IR spectra of BA-NE mixtures with aromatic rings, both the peaks corresponding to the stretching mode of the aromatic ring (1500-1650 cm^{-1}) and the C-H out-of-plane mode of the aromatic ring (800-900 cm^{-1}) are blue-shifted.[27] These results suggest that the aromatic rings of BA interact with NE. The positive change of Δ $\tilde{\nu}$ (PO_2^-) for DOPC-NA and DOPC-DA mixtures with the addition of CA suggests that the CA molecules are additionally adsorbed onto DOPC-NA and DOPC-DA mixed molecular layers (Figures 3b2 and 3b4). The slight change of Δ $\tilde{\nu}$ (PO_2^-) for DOPC-NA and DOPC-DA upon addition of BA suggests that BA molecules have little effect on DOPC-NA and DOPC-DA mixed molecular layers (Figures 3b2 and 3b4).

The experimental results for the *Π-A* isotherms and FT-IR spectra are summarized in Table 1. For TS molecules with double bonds, that is, NE and DE, the effect of OD molecules on the DOPC-TS mixed layer was roughly classified by the presence or absence of a benzene ring in the OD molecules. For TS molecules with double bonds, that is, NE and DE, OD molecules with a benzene ring affect TS desorption but have little effect on TS molecules without double bonds, that is, NA and DA.

Table 1. Comparison between DOPC-TS-OD mixed molecular layer and DOPC-TS molecular layer concerning Parameters ΔA and $\Delta\,\tilde{\nu}\,(PO_2^-)$. $\Delta A = \Delta A_{\text{DOPC-TS-OD}} - \Delta A_{\text{DOPC-TS}}$ (Figure 2), and $\Delta\,\tilde{\nu}\,(PO_2^-) = \tilde{\nu}_{\text{DOPC-TS-OD}} - \tilde{\nu}_{\text{DOPC-TS}}$ (Figure 3).

	Target substances	Parameter	BA (with benzene ring)	CA (without benzene ring)
With double bond	NE (C=9)	ΔA	− 10.9	+ 2.8
		$\Delta\tilde{\nu}$	− 1.7	+ 0.5
	DE (C=10)	ΔA	− 2.5	+ 1.7
		$\Delta\tilde{\nu}$	− 3.6	− 0.8
Without double bond	NA (C=9)	ΔA	+ 6.7	+ 16.7
		$\Delta\tilde{\nu}$	− 0.2	+ 2.5
	DA (C=10)	ΔA	− 2.0	+ 2.4
		$\Delta\tilde{\nu}$	0	+ 2.4

CONCLUSIONS

ΔA of the *Π-A* isotherm for DOPC was significantly higher for TS molecules with double bonds than for TS molecules without double bonds. In addition, ΔA for DOPC-NE and DOPC-DE mixed molecular layers characteristically changed depending on the chemical structure of OD molecules, i.e., OD molecules with an aromatic ring revealed a lower ΔA, but OD molecules without an aromatic ring induced similarly high ΔA. The characteristic responses of the DOPC molecular layer to OD molecules were discussed in terms of the interactions between DOPC, TS, and OD molecules based on the ATR-FT-IR results. The decrease in the wavenumber of the PO_2^- antisymmetric stretch mode of the DOPC-NE

and DOPC-DE mixed films with the addition of BA indicated that BA played an important role in the desorption of these TS molecules from the DOPC-TS mixed films. In addition, the experimental results seem to be related to the responses of skin to odors, i.e., the difference in the cytotoxicity with or without double bonds of TS molecules.[10] OD molecules with benzene rings are useful for masking these effects. This study is useful for understanding the mechanisms of the masking effects observed on lipid membranes, without considering olfactory receptors from view point of molecular structure. In this study, DOPC was selected as an artificial lipid membrane system. However, the actual cell membranes contain cholesterol and other phospholipids, e.g., phosphatidylserine and phosphatidylethanolamine.[30] Similar experiments using other phospholipids or cholesterol-containing membranes may induce characteristic responses to chemical stimuli. Based on the present study, we can elucidate the detailed mechanisms by which odor molecules affect lipid membranes without mediating olfactory receptors and develop more effective OD molecules with a masking effect.

ASSOCIATED CONTENT

Supporting Information

The Supporting Information is available free of charge at

https://pubs.acs.org/doi/10.1021/acs.langmuir....

FT-IR spectra of DOPC, DOPC-TS, DOPC-TS-OD mixtures are shown in Figure S1. FT-IR spectra for DOPC, DOPC-TS, and DOPC-TS-OD mixtures around PO_2^- antisymmetric stretching region (~1240 cm^{-1}) and their analytical procedures to obtain the wavenumber at IR absorbance peak arising from the PO_2^- antisymmetric stretch vibration mode of DOPC are shown in Figure S2. *Π-A* isotherms for TS and OD developed on water as a single sample are shown in Figure S3.

AUTHOR INFORMATION

Corresponding Author

Satoshi Nakata − Graduate School of Integrated Sciences for Life, Hiroshima University, Higashi-Hiroshima 739-8526, Japan; orcid.org/0000-0002-7290-1508; Phone: +81-824-24-7409; E-mail: nakatas@hiroshima-u.ac.jp

Authors

Mai Yotsumoto − Graduate School of Integrated Sciences for Life, Hiroshima University, Higashi-Hiroshima 739-8526, Japan

Risa Fujita − Graduate School of Integrated Sciences for Life, Hiroshima University,

Higashi-Hiroshima 739-8526, Japan

Muneyuki Matsuo − Graduate School of Integrated Sciences for Life, Hiroshima University, Higashi-Hiroshima 739-8526, Japan /Graduate School of Arts and Sciences, The University of Tokyo, 3-8-1 Komaba, Meguro-ku, Tokyo, 153-8902, Japan; orcid.org/0000-0002-2559-3522

Shinobu Nakanishi − Shiseido Global Innovation Center, 1-2-11 Takashima-cho, Nishi-ku, Yokohama, Kanagawa 220-0011, Japan

Mitsuhiro Denda − Meiji University Institute for Advanced Study of Mathematical Sciences, 8F High-Rise Wing, Nakano Campus, Meiji University, 4-21-1 Nakano, Nakano-ku, Tokyo, 164-8525, Japan

Author Contributions

Satoshi Nakata supervised the research; Mai Yotsumoto and Risa Fujita performed the experiments and analyzed the data; Mai Yotsumoto wrote the paper, and all authors revised the manuscript and discussed the present study.

Funding

This study was supported by JSPS KAKENHI (Grant No. JP20H02712, JP21H00996), Iketani Science and Technology Foundation, the Cooperative Research Program of

"Network Joint Research Center for Materials and Devices" (No. 20231004), to S. N., and the JSPS Bilateral Joint Research Project between Japan and the JSPS-Hungary Bilateral Joint Research Project (JPJSBP120213801). This study was supported by a Sasakawa Scientific Research Grant from the Japan Science Society awarded (No. 2023-6004) and JST, the establishment of university fellowships towards the creation of science technology innovation (JPMJFS2129) to M. Y.

Notes

The authors declare no competing financial interest.

REFERENCES

(1) Hirasawa, Y.; Shirasu, M.; Okamoto, M.; Touhara, K. Subjective Unpleasantness of Malodors Induces a Stress Response. *Psychoneuroendocrinology* **2019**, *106,* 206-215.

(2) Masuo, Y.; Satou, T.; Takemoto, H.; Koike, K. Smell and Stress Response in the Brain: Review of the Connection between Chemistry and Neuropharmacology. *Molecules* **2021**, *26*, 2571.

(3) Horton, R. A.; Wing, S.; Marshall, S. W.; Brownley, K. A. Malodor as a Trigger of Stress and Negative Mood in Neighbors of Industrial Hog Operations. *Am. J. Public Health* **2009**, *99*, 610-615.

(4) Schiffman, S. S.; Williams, C. M. Science of Odor as a Potential Health Issue. *J. Environ. Qual.* **2005**, *34*, 129-138.

(5) Conti, C.; Guarino, M.; Bacenetti, J. Measurements Techniques and Models to Assess Odor Annoyance: A Review. *Environ. Int.* **2020**, *134*, 105261.

(6) Palmiotto, M.; Fattore, E.; Paiano, V.; Celeste, G.; Colombo, A.; Davoli, E. Influence of a Municipal Solid Waste Landfill in the Surrounding Environment: Toxicological Risk and Odor Nuisance Effects. *Environ. Int.* **2014**, *68*, 16-24.

(7) Haze, S.; Gozu, Y.; Nakamura, S.; Kohno, Y.; Sawano, K.; Ohta, H. 2-Nonenal Newly Found in Human Body Odor Tends to Increase with Aging. *J. Invest. Dermatol.* **2001**, *116*, 520-524.

(8) Yamazaki, S.; Hoshino, K.; Kusuhara, M. Odor Associated with Aging. *Anti-Aging Med.* **2010**, *7*, 60-65.

(9) Ghadially, R.; Brown, B. E.; Sequeira-Martin, S. M.; Feingold, K. R.; Elias, P. M. The aged epidermal permeability barrier. Structural, functional, and lipid biochemical abnormalities in humans and a senescent murine model. *J. Clin. Investig.* **1995**, *95*, 2281-2290.

(10) Nakanishi, S.; Makita, M.; Denda, M.; Effects of *trans*-2-Nonenal and Olfactory Masking Odorants on Proliferation of Human Keratinocytes. *Biochem. Biophys. Res.*

Commun. **2021**, *548*, 1-6.

(11) Takeuchi, H.; Ishida, H.; Hikichi, S.; Kurahashi, T. Mechanism of Olfactory Masking in the Sensory Cilia. *J. Gen. Physiol.* **2009**, *133*, 583-601.

(12) Zhuang, L.; Wei, X.; Jiang, N.; Yuan, Q.; Qin, C.; Jiang, D.; Mengxue, L.; Yanning, Z.; Wang, P. A Biohybrid Nose for Evaluation of Odor Masking in the Peripheral Olfactory System. *Biosens. Bioelectron.* **2021**, *171*, 112737.

(13) Lenochová, P.; Vohnoutova, P.; Roberts, S. C.; Oberzaucher, E.; Grammer, K.; Havlíček, J. Psychology of Fragrance Use: Perception of Individual Odor and Perfume Blends Reveals a Mechanism for Idiosyncratic Effects on Fragrance Choice. *PloS One* **2012**, *7*, 33810.

(14) Wysocka, I.; Gębicki, J.; Namieśnik, J. Technologies for Deodorization of Malodorous Gases. *Environ. Sci. Pollut. Res.* **2019**, *26*, 9409-9434.

(15) Sanhueza. M.; Bacigalupo, J. Odor Suppression of Voltage-Gated Currents Contributes to the Odor-Induced Response in Olfactory Neurons. *Am. J. Physiol.* **1999**, *277*, C1086-C1099.

(16) Oshima, A.; Nakanishi, K.; Kasai, N.; Nakashima, H.; Tsumoto, K.; Sumitomo, K.; Mechanism of Budded Virus Envelope Fusion into a Planar Bilayer Lipid Membrane on a SiO_2 Substrate. *Langmuir*, **2022**, *38*, 5464-5471.

(17) Ma, T.; Sato, M.; Komiya, M.; Feng, X.; Tadaki, D.; Hirano-Iwata, A. Advances in Artificial Bilayer Lipid Membranes as a Novel Biosensing Platform: From Drug-screening to Self-assembled Devices. *Chem. Lett.* **2021**, *50*, 418-425.

(18) Tameyuki, M.; Hiranaka, H.; Toyota, T.; Asakura, K.; Banno, T.;Temperature-Dependent Dynamics of Giant Vesicles Composed of Hydrolysable Lipids Having an Amide Linkage. *Langmuir*, **2019**, *35*, 17075-17081.

(19) Kobayashi, M.; Noguchi, H.; Sato, G.; Watanabe, C.; Fujiwara, K.; Yanagisawa, M. Phase-Separated Giant Liposomes for Stable Elevation of α-Hemolysin Concentration in Lipid Membranes. *Langmuir* **2023**, *39*, 11481-11489.

(20) Chattaraj, R.; Blum, N. T.; Goodwin, A. P. Design and application of stimulus-responsive droplets and bubbles stabilized by phospholipid monolayers. *Curr. Opin. Colloid Interface Sci.* **2019**, *40*, 14-24.

(21) Denda, M.; Umino, Y.; Kumazawa, N.; Nakata, S. Can simple physicochemical studies predict the effects of molecules on epidermal water-impermeable barrier function? *Exp. Dermatol.* **2022**, *29*, 393-399.

(22) Brady, J. D.; Rich, T. C.; Le, X.; Stafford, K.; Fowler, C. J.; Lynch, L.; Karpen, J. W.; Brown, R. L.; Martens, J. R. Functional Role of Lipid Raft Microdomains in Cyclic Nucleotide-Gated Channel Activation. *Mol. Pharmacol.* **2004**, *65*, 503-511.

(23) Lowry, T. W.; Kusi-Appiah, A. E.; Fadool, D. A.; Lenhert, S. Odor Discrimination by Lipid Membranes. *Membranes* **2023**, *13*, 151.

(24) Nomura, T.; Kurihara, K. Effects of changed lipid composition on responses of liposomes to various odorants: possible mechanism of odor discrimination. *Biochemistry* **1987**, *26*, 6141-6145.

(25) Kashiwayanagi, M.; Suenaga, A.; Enomoto, S.; Kurihara, K. Membrane fluidity changes of liposomes in response to various odorants. Complexity of membrane composition and variety of adsorption sites for odorants. *Biophys. J.* **1990**, *58*, 887-895.

(26) Fujita, R.; Yotsumoto, M.; Yamaguchi, Y.; Matsuo, M.; Fukuhara, K.; Takahashi, O.; Nakanishi, S.; Denda, M.; Nakata, S. Masking of a Malodorous Substance on 1, 2-Dioleoyl-*sn*-glycero-3-phosphocholine Molecular Layer. *Colloids Surf. A* **2022**, *634*, 128045.

(27) Jha, S. K. Characterization of human body odor and identification of aldehydes using chemical sensor. *Rev. Anal. Chem.* **2016**, *36*, 20160028.

(28) Adrian, C.; Szuwarzyński, M.; Kwolek, U.; Wydro, P.; Kepczynski, M.; Zapotoczny, S.; M. Nowakowska, Quaroni, L. Label-Free Infrared Spectroscopy and Imaging of Single Phospholipid Bilayers with Nanoscale Resolution. *Anal. Chem.* **2018**, *90*, 10179-10186.

(29) Kishino, Y.; Kato, H.; Kurahashi, T.; Takeuchi, H. Chemical Structures of Odorants that Suppress Ion Channels in the Olfactory Receptor Cell. *J. Physiol. Sci.* **2011**, *61*, 231-245.

(30) Spector, A. A.; Mark A. Y. Membrane lipid composition and cellular function. *J. Lipid Res.* **1985**, *26*, 1015-1035.